

# Mesospheric observations **and** modeling **of the** Zeeman **split** 233.9 GHz $^{18}\text{O}^{16}\text{O}$ line

Brad .I. Sandor<sup>1</sup> and R. Todd Clancy<sup>2</sup>

Received \_\_\_\_\_; accepted \_\_\_\_\_

Short title:  $^{18}\text{O}^{16}\text{O}$  MICROWAVE OBSERVATION IN MESOSPHERE

<sup>1</sup> JetPropulsion Laboratory, California Institute of Technology, Pasadena

<sup>2</sup>Space Science Institute, Boulder, Colorado

# **Abstract.**

Observations made from Kitt Peak, AZ, of the 233.9 GHz emission line of  $^{18}\text{O}^{16}\text{O}$  in the upper stratosphere and lower mesosphere are reported. A good model fit to the line is obtained by incorporation of pressure and temperature broadening effects, as well as a Zeeman splitting algorithm that uses a standard geomagnetic field model and a paramagnetic Hamiltonian description of the molecular energy states. These observations are used, along with the well known  $^{18}\text{O}^{16}\text{O}$  mixing ratio, to establish absolute calibration for observations of other chemical species from Kitt Peak. Repeated measurements show 110 change in this absolute calibration] between observation dates. The wide magnetic splitting ( $\pm 1.8$  MHz) exhibited by this line with only six Zeeman components [J1'o~'ides a unique test of middle atmosphere Zeeman effect model calculations, supporting the use of  $\text{O}_2$  lines by microwave atmospheric sounders to measure pressure and temperature.

## 1. Introduction

We are conducting an ongoing program [Clancy *et al.*, 1994, and references therein] of ground-based microwave observations of blackbody line emissions from trace atmospheric chemical species in Earth's upper stratosphere, mesosphere, and lower thermosphere. Abundance of an observed species is determined from the intensity of its emission, where each observation is of column emission along a line of sight at fixed elevation and azimuth. Altitude distribution of the radiating species is determined from the shape of its emission line, which is controlled by the dependence of pressure (collisional) broadening on altitude [Clancy and Muhleman 1993]. Frequency switching is used to remove the background signal, and makes the data insensitive to the very broadband emission from below 40 km. The upper limit to the altitude range represented by the data is set by the decrease in number density with increasing altitude.  $^{18}\text{O}^{16}\text{O}$  observations presented here are sensitive to emissions from 45–70 km altitude.

As part of the calibration procedure, the 233.9 GHz line of  $^{18}\text{O}^{16}\text{O}$  was observed. This line is an ideal calibrator because its mixing ratio in the atmosphere is well known [Kroopnick and Craig, 1972] and constant with altitude [Dole *et al.* 1954]. Splitting of the 233.9 GHz  $^{18}\text{O}^{16}\text{O}$  Zeeman components also provides a measure of magnetic field effects, which are important for interpretation of 255.0 GHz  $\text{O}_2(^1\Delta_g)$  observations [Sandor *et al.* 1997].

[Hartmann *et al.*, 1996] describe their Millimeter-wave Atmospheric Sounder (MAS) observations of the Zeeman-split 61.15 GHz  $\text{O}_2$  line in the mesosphere. MAS is one component of the NASA Space Shuttle ATLAS missions. They report an observed Zeeman-splitting width at 80 km altitude which is smaller than that predicted from theory. This discrepancy is important because  $\text{O}_2$  microwave emissions are used to measure temperature and pressure in the middle atmosphere up to 0.46 hPa ( $\sim 55$  km) [Fishbein *et al.*, 1996], and will be used in the future for such measurements at higher altitudes where an accurate Zeeman splitting calculation becomes more important. In particular, the

Earth Observing System Microwave Limb Sounder (EOS MLS) will observe the 233.9 GHz  $^{18}\text{O}^{16}\text{O}$  line to provide temperature and pressure measurements over part of the instrument's vertical range [*J. Waters, private communication 1997*]. We report a 233.9 GHz  $^{18}\text{O}^{16}\text{O}$  magnetic splitting width that agrees with theory, and discuss below the implications this has for understanding the [*Hartmann et al., 1996*] 61.15 GHz  $\text{O}_2$  discrepancy.

## 2. Spectroscopy

The  $^{18}\text{O}^{16}\text{O}$  line emission at 233.94618 GHz is a magnetic dipole,  $(N=2, J=1) \rightarrow (N=0, J=1)$ , rotational transition with Zeeman splitting due to the net electron spin ( $S=1$ ) of the molecule, into six linearly polarized components. Line center frequency and integrated line strength were obtained from the 1996 edition of the HITRAN spectroscopy catalogue [*Poynter and Pickett 1985; Pickett et al., 1996*]. The collisional (pressure) broadening coefficient used was 1.93 MHz/hPa, based on  $^{16}\text{O}^{16}\text{O}$  laboratory measurements [*Liebe et al. 1992*].

Four of the Zeeman components are polarized perpendicular, and two parallel, to the Earth's magnetic field. The energy shift of each quantum state due to the geomagnetic field ( $B$ ) is given by:

$$\Delta E = g\mu_0 M_J B \quad (1)$$

where  $\mu_0$  is the Bohr magneton. Frequency offset of a Zeeman component from line center is determined by subtracting  $\Delta E$  of the lower state from  $\Delta E$  of the upper state and dividing by Planck's constant.  $g = 1.001 \frac{J(J+1) + S(S+1) - N(N+1)}{J(J+1)}$  corresponds to the vector model approximation [*Townes and Schawlow, 1955*]. The vector model would give  $g$  values of -1.001 and 2.002 for the upper and lower states, respectively, leading to a 13% error in the 233 GHz  $^{18}\text{O}^{16}\text{O}$  splitting. We calculate the splitting more exactly by

following the formulation of *Mizushima* [1975], in which each quantum state is written as a linear combination of states  $N$  and  $N\pm 2$ , the paramagnetic Hamiltonian is calculated, and the secular equation is solved. This leads to  $g$  values of  $-0.818$  and  $1.821$  for the  $(N=2, J=1)$  and  $(N=0, J=1)$  states, respectively, and to agreement between observed and modeled Zeeman splitting widths. Relative emission strengths of the Zeeman components were calculated according to *Townes and Schawlow* [1955].

### 3. Observations

Observations of  $^{18}\text{O}^{16}\text{O}$  at 233.94618 GHz were made from Kitt Peak Arizona ( $32^\circ\text{N}$ ,  $112^\circ\text{W}$ ), using the National Radio Astronomy Observatory (NRAO)<sup>3</sup> 12-meter radio telescope and microwave receivers.

Microwave spectra of  $^{18}\text{O}^{16}\text{O}$  were obtained in the frequency switched mode at fixed elevation ( $20^\circ$ ,  $30^\circ$  or  $90^\circ$ ) and azimuth ( $270^\circ$  or  $90^\circ$ ). Details of the frequency switched observations can be found in discussion of similar NO [*Clancy et al.*, 1992] and  $\text{HO}_2$ ,  $\text{O}_3$ , and  $\text{H}_2^{18}\text{O}$  [*Clancy et al.*, 1994] Kitt Peak measurements. A best fit to each spectrum was found using an iterative least squares procedure to minimize differences between the data and a synthetic 233.9 GHz  $^{18}\text{O}^{16}\text{O}$  line. Observed spectral brightness temperatures are roughly linearly proportional to the  $^{18}\text{O}^{16}\text{O}$  abundances within the 45-70 km altitude region. Figure 1 shows representative differences of the normalized weighting functions; all such difference functions peak between 46 and 68 km, indicating the altitude range to which the observation is sensitive.

Simultaneous observations were made with two orthogonal, linearly polarized receivers, and signals from these receivers were saved separately. Because the receiver polarization axes are in general not aligned with the geomagnetic field, each receiver

<sup>3</sup>The National Radio Astronomy Observatory is operated by Associated Universities, Inc., under cooperative agreement with the National Science Foundation.

records a signal with contributions from all six of the line's Zeeman components. As part of the data analysis procedure, the relative contributions of perpendicular and parallel line components to each receiver's detection are worked out, based on the direction of the geomagnetic field, telescope pointing direction, and the orientation of the telescope receivers. Magnetic field data were taken from the 1987 International Geomagnetic Reference Field (IGRF) [Barraclough 1987].

Because the Zeeman components polarized parallel to  $\mathbf{B}$  exhibit the largest frequency shifts, and because there are only two lines at this polarization, it is the parallel polarization which provides the most sensitive test of the Zeeman splitting model and illustration of line splitting. Figure 2 presents an observation made at  $90^\circ$  azimuth,  $20^\circ$  elevation, for which 82% of the signal (in one of the receivers) is from parallel-polarized emission. For this observation geometry from Kitt Peak, IGRF specifies a field magnitude at 65 km altitude of  $0.472 \pm 0.003$  G, where the uncertainty is based on variation of the field along the line of sight. Figure 3 presents the spectrum observed simultaneously with that of figure 2, but at orthogonal polarization, such that only 10% of the signal is from parallel-polarized emission. Observations for geometries dominated by the widely split parallel-polarized Zeeman components are listed in Table 1. As a measure of the consistency of the Zeeman splitting and magnetic field models, the magnetic field intensity for each of these observations was varied during the data reduction procedure to obtain a best fit to each spectrum. These best-fit values for  $B$  deviate from the IGRF values by no more than 2%, indicating the Zeeman splitting and magnetic field are well understood. Agreement between the model and best-fit values of  $B$  is equivalent to agreement between the model and best-fit frequency separation due to Zeeman splitting.

## 4. Results and Discussion

Data obtained January 14, 1994 and a synthetic best fit line are presented in figures 2 and 3. Data have been collected over a period of more than three years, at different

times of day and for different observation geometries (i.e. telescope pointing directions). There was no significant variation in signal between same-geometry observations, from which we conclude there has been no drift in instrument calibration. Fitting data to the known  $^{18}\text{O}^{16}\text{O}$  abundance from  $90^\circ$  elevation observations requires  $T_{\text{B}}$  to be multiplied by  $0.70 \pm 0.03$ , where the uncertainty was estimated by inverting the data for 5 K perturbations to the climatological [Rees *et al.*, 1990] temperature profiles, and for a 5% perturbation to the pressure broadening coefficient.  $1-\sigma$  uncertainty due to noise was less than 1%. This  $0.70 \pm 0.03$  absolute calibration factor is consistent with the theoretical factor 0.68 at zenith [P. Jewell, *private communication*], which follows from the atmosphere filling  $2\pi$  steradians of sky and the use of hard coded calibration at Kitt Peak that was determined for observation of small angular size astronomical objects. Manual tip observations of CO at 230 GHz and O<sub>3</sub> at 249 and 210 GHz, which serve as the primary means to characterize the elevation-angle dependence of the calibration, indicate a  $20^\circ$  elevation factor of  $0.84 \pm 0.04$ . 233.9 GHz  $^{18}\text{O}^{16}\text{O}$  data at  $20^\circ$  elevation require a calibration factor of  $0.81 \pm 0.06$ , in agreement with the CO and O<sub>3</sub> manual tip results. These empirical  $20^\circ$  calibrations are consistent with theory, which predicts a calibration factor of 0.84 at  $0^\circ$  elevation.

Hartmann *et al.* [1996] observed Zeeman splitting of the 61 GHz ( $9^+$ ) O<sub>2</sub> line, using the Millimeter-wave Atmospheric Sounder, which was part of the NASA Space Shuttle Atlas payload. They report a narrower line width than expected for emissions from 80 km altitude. Hartmann *et al.* [1996] use the Liebe *et al.* [1993] Zeeman Propagation Model, which assumes [Liebe, 1981] the vector model of Zeeman splitting. However, unlike the 233.9 GHz  $^{18}\text{O}^{16}\text{O}$  line described here, the vector model is very accurate for the O<sub>2</sub> 61 GHz line. Hartmann *et al.* [1996] suggest interference between overlapping Zeeman line components as one possible explanation for their splitting width discrepancy. This suggestion is consistent with the agreement of our observed and modeled line widths, because the 6 components of the 233.9 GHz  $^{18}\text{O}^{16}\text{O}$  line have an order of magnitude more

separation between adjacent components than the 57 components of the 61 GHz O<sub>2</sub> line. The 233.9 GHz <sup>18</sup>O<sup>16</sup>O line is thus less sensitive than the 61 GHz O<sub>2</sub> line to interference between Zeeman line components. The 233.9 GHz <sup>18</sup>O<sup>16</sup>O and 61 GHz O<sub>2</sub> line fitting procedures are equally sensitive to errors in the IGRF model magnetic field. Thus from work presented here we argue the IGRF accurately represents the geomagnetic field in the mesosphere, and that the *Hartmann et al.* [1996] Zeeman width discrepancy is not due to any error in the magnetic field model.

## 5. Summary

The 233.9 GHz <sup>18</sup>O<sup>16</sup>O line has been observed in emission from the lower mesosphere and upper stratosphere. The data is well fit with a synthetic line calculation that includes pressure and Doppler broadening, as well as Zeeman splitting in the geomagnetic field. This work verifies Zeeman model calculations for oxygen in the mesosphere, clarifies the *Hartmann et al.* [1996] analysis of 61 GHz O<sub>2</sub> MAS observations, and supports the use of O<sub>2</sub> microwave observations to measure temperature and pressure in the middle atmosphere. Our 233.9 GHz <sup>18</sup>O<sup>16</sup>O results support the [*Hartmann et al.*, 1996] suggestion that the discrepancy between their observed and modeled 61 GHz O<sub>2</sub> line width is caused by interference among Zeeman components of the 61 GHz O<sub>2</sub> line. The 233.9 GHz <sup>18</sup>O<sup>16</sup>O observations have been used in a calibration procedure for ground-based microwave observations of the atmosphere.

**Acknowledgments.** We gratefully acknowledge the assistance of NRAO staff at Kilt Peak, in particular that of telescope operators Duane Clark, Lisa Engel, Paul Hart, Harry Stahl, and Ed Treiber. We thank Ed Cohen, Phil Jewell, Ted Lungu, and Ted Speiser for scientific and technical discussions. The research described in this paper was partially performed while 11.1. Sandor held a National Research Council-NASA Resident Research Associateship award at the Jet Propulsion Laboratory, California Institute of Technology, under contract with the National Aeronautics and Space Administration.

## References

- Barracough, D.H., International Geomagnetic Reference Field: The fourth generation, *Phys. Earth Planet. Inter.*, **48**, 279-292, 1987.
- Clancy, R.T., D. W. Rusch, and D.O. Muhleman, A microwave measurement of high levels of thermospheric nitric oxide, *Geophys. Res. Lett.*, **19**, 261-264, 1992.
- Clancy, R.T., and D.O. Muhleman, Ground-based microwave spectroscopy of the earth's stratosphere and mesosphere, in *Atmospheric Remote Sensing by Microwave Radiometry*, edited by M. A. Janssen, pp. 335-352. John Wiley, New York, 1993.
- Clancy, R.T., B.J. Sandor, D. W. Rusch, and D.O. Muhleman, Microwave observations and modeling of O<sub>3</sub>, H<sub>2</sub>O, and HO<sub>2</sub> in the mesosphere, *J. Geophys. Res.*, **99**, 5465-5473, 1994.
- Dole, M., G.A. Lane, D.P. Rudd, and D.A. Zaukelies, Isotopic Composition of Atmospheric Oxygen and Nitrogen, *Geochim. Cosmochim. Acta.* **4**, 65-78, 1954.
- Fishbein, E.F., R.E. Cofield, L. Froidevaux, R.F. Jarnot, T. Lungu, W.G. Read, Z. Shippony, J. W. Waters, I. S. McDermid, T.J. McGee, U. Singh, M. Gross, A. Hauchecorne, P. Keckhut, M.E. Gelman, and R.M. Nagatani, Validation of UARS Microwave Limb Sounder temperature and pressure measurements, *J. Geophys. Res.*, **101**, 9983-10,016, 1996.
- Hartmann, G. K., W. Degenhardt, M.L. Richards, H.J. Liebe, G.A. Hufford, M.G. Cotton, R. M. Bevilacqua, J. J. Olivero, N. Kampfer, and J. Langen, Zeeman splitting of the 61 Gigahertz Oxygen (O<sub>2</sub>) line in the mesosphere, *Geophys. Res. Lett.*, **23**, 2329-2332, 1996.
- Kroopnick, P., and H. Craig, Atmospheric oxygen: Isotopic composition and solubility fractionation, *Science*, **175**, 54-55, 1972.
- Liebe, H.J., Modeling attenuation and phase of radio waves in air at frequencies below 1000 GHz, *Radio Sci.*, **16**, 1183-1199, 1981.
- Liebe, H. J., P. Y. Rosenkranz, and G.A. Hufford, Atmospheric 60-GHz oxygen spectrum: New laboratory measurements and line parameters, *J. Quant. Spectrosc. Radiat. Transf.*, **48**, 629-643, 1992.
- Liebe, H.J., G.A. Hufford, and M.G. Cotton 1993. Propagation modeling of moist air and suspended water/ice particles at frequencies below 1000 GHz. *AGARD CP- 542*, **3**, Mallorca.

Spain.

- Mizushima, M., *The Theory of Rotating Diatomic Molecules*, 543 pp., John Wiley and Sons, 1975.
- Pickett, H.M., R.L. Poynter, E.A. Cohen, M.L. Delitsky, J.C. Pearson, and H.S.P. Muller, *Submillimeter, Millimeter, and Microwave Spectral Line Catalog, JPL Publ. 80-23*, Jet Propul. Lab., Pasadena, Calif., 1996.
- Poynter, R.L., and H.M. Pickett, Submillimeter, millimeter, and microwave spectral line catalog, *Appl. Opt.*, 24, 2235-2240, 1985.
- Rees, D., J.J. Barnett, and K. Labitzke (eds.), *Advances in Space Research, vol 10. COSPAR International Reference Atmosphere: 1986; Part II: Middle Atmosphere*, 519 pp., Pergamon Press, 1990.
- Sandor, B.J., R.T. Clancy, D.W. Rusch, C.E. Randall, R.S. Eckman, D.S. Siskind, and D.O. Muhleman, Microwave Observations and Modeling of  $\text{O}_2(^1\Delta_g)$  and  $\text{O}_3$  Diurnal Variation in the Mesosphere, *J. Geophys. Res.*, in press, 1997.
- Townes, C.H., and A.L. Schawlow, *Microwave Spectroscopy*, 698 pp., McGraw-Hill Company, 1955.

**Table 1.** 233.9 GHz  $^{18}\text{O}^{16}\text{O}$  observation dates for geometries dominated by parallel-polarized emission. Best fit values of B are within 2% of the IGRF value 0.472 G, indicating Zeeman splitting in the geomagnetic field is well understood. Results are consistent for all seasons, times of day, and under the wide variety of observing weather conditions indicated by the  $T_{\text{sys}}$  values.

**Figure 1.** Relative weighting functions for the observed  $^{18}\text{O}^{16}\text{O}$  spectrum (Figure 2). Each curve represents the **altitude profile of the sensitivity of line pair signal differences to  $^{18}\text{O}^{16}\text{O}$  abundance.** For example, the frequency pair 1.45- 2.45 corresponds to the difference between line emission observed at 1.45 and 2.-1.5 MHz from line center and **is most sensitive to emission from  $^{18}\text{O}^{16}\text{O}$  at altitudes of 50-70 km.** These weighting functions have units of (mixing ratio) $^{-1}$ .

**Figure 2.** 233.9 GHz spectrum of  $^{18}\text{O}^{16}\text{O}$ , observed January 24, 1994, 4:35-5:05pm, local time. Vertical lines indicate relative contribution of the **six Zeeman components to the line.** For **this geometry, the spectrum is dominated by the two parallel-polarized components with separation 3.5 MHz.** Negative **features** near  $\pm 6$  MHz are artifacts of the frequency switching procedure used **for** baseline subtraction.

**Figure 3.** 233.9 GHz spectrum of  $^{18}\text{O}^{16}\text{O}$  observed simultaneously with that of figure 2, but at orthogonal polarization. Vertical lines indicate relative contribution of the six Zeeman components to the line. For this geometry, the spectrum is dominated by the four perpendicular-polarized components. Negative features near  $\pm 5$  MHz are artifacts of the frequency switching procedure used for baseline subtraction.

Table 1

Date	Time, MST	Elev.	Az.	% Parallel	% Perp.	B (Gauss)	T <sub>sys</sub> (K)
<b>Nov 27, 1993</b>	2009-2021	30°	90°	79	21	0.476	653
Jan 14, 1994	1635-1703	20°	90°	82	18	0.481	1480
Dec 3, 1995	0527-0737	20°	90°	82	18	0.479	1583
<b>Jan 16, 1996</b>	1736-1810	20°	90°	82	18	0.475	3396
<b>Jan 25, 1997</b>	1600-1638	30°	90°	79	21	0.470	2856

Fig. 1:  $^{18}\text{O}^{16}\text{O}$  233 GHz Weighting Functions

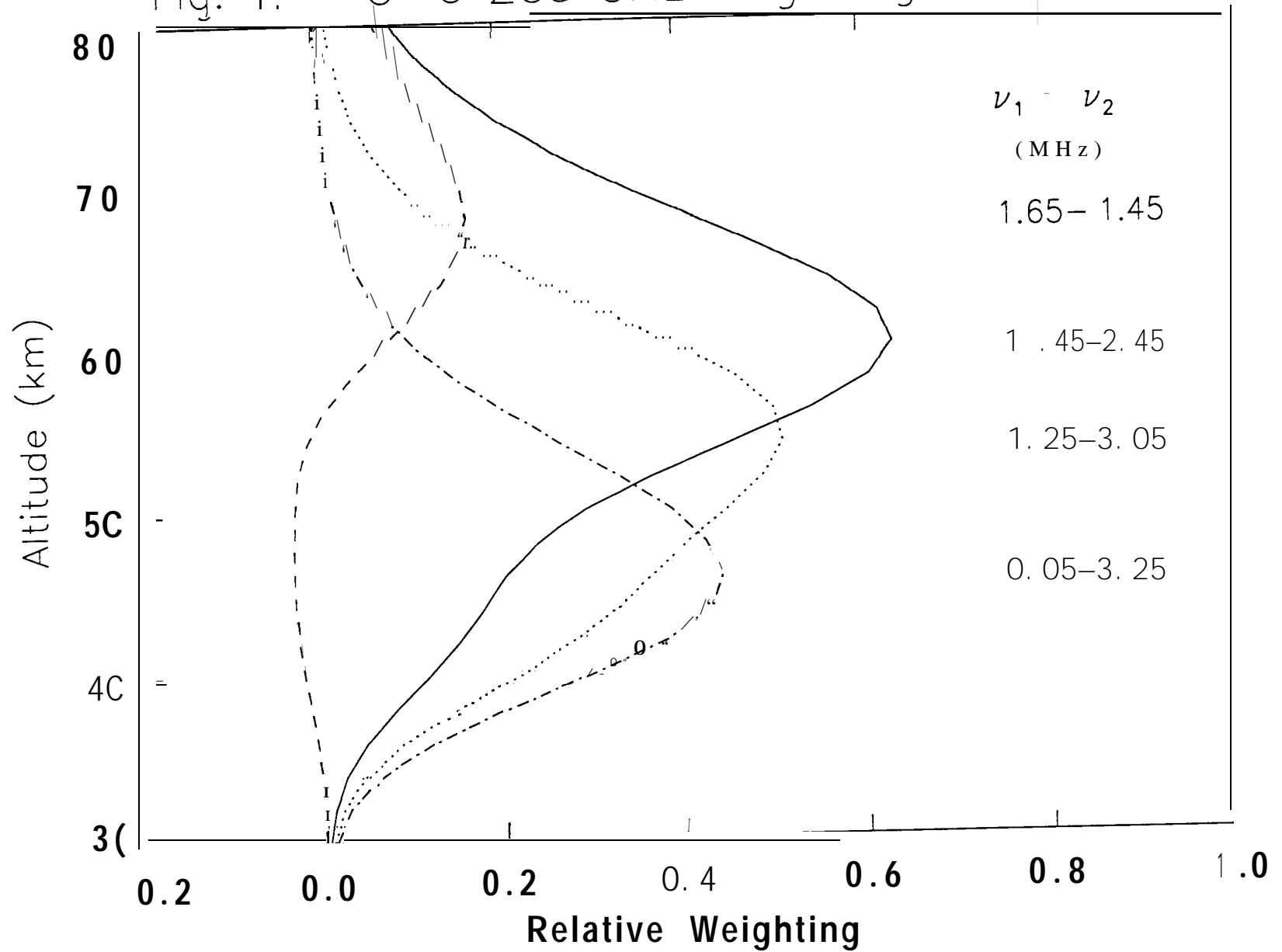


Fig 2: 233.9GHz  $^{18}\text{O}^{16}\text{O}$ , 14Jan94

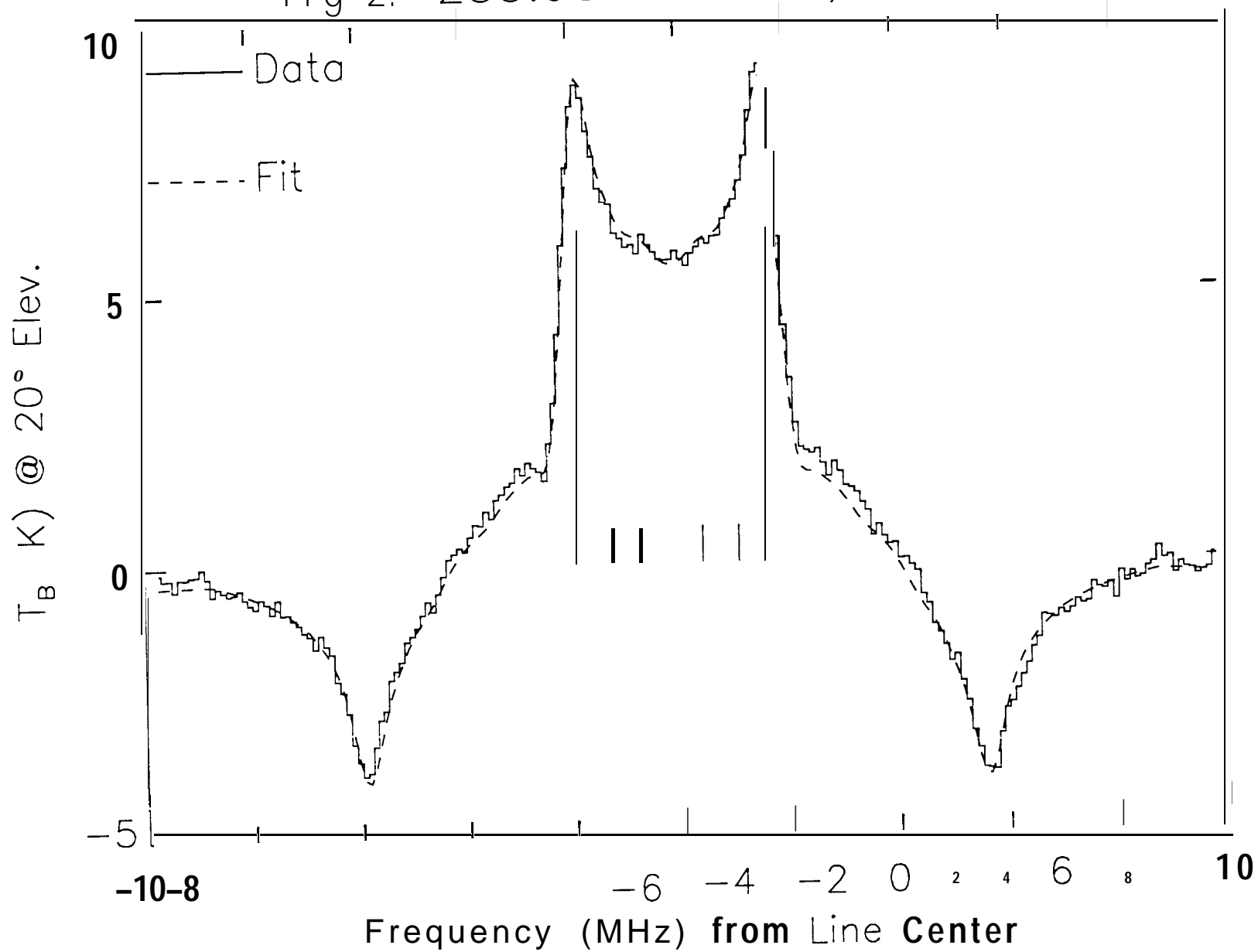


Fig 3: 233.9GHz  $^{18}\text{O}^{16}\text{O}$  14Jan94

